Circular waveguides induced by two-dimensional bright steady-state photorefractive spatial screening solitons

Ming-feng Shih and Mordechai Segev

Department of Electrical Engineering and Center for Photonics and Optoelectronics Materials, Princeton University, Princeton, New Jersey 08544

Greg Salamo

Department of Physics, University of Arkansas, Fayetteville, Arkansas 72701

Received February 20, 1996

We report what we believe is the first experimental observation of bright-soliton-induced two-dimensional waveguides. The waveguides are induced by two-dimensional photorefractive screening solitons, and their guiding properties, i.e., whether the waveguides are single mode or multimode, are controlled by adjustment of the soliton parameters. © 1996 Optical Society of America

Recently spatial solitons have been attracting much research activity. Potential applications of spatial solitons, such as controlling and manipulating light by light, are now becoming feasible. Bright Kerr-type solitons have been investigated for years.[1,2] However, they are inherently unstable in a bulk medium and thus can be observed only in a planar waveguide,[2] implying that all potential device applications must be planar. Furthermore Kerr self-focusing of a two-dimensional beam leads not to solitons but rather to catastrophic self-focusing.[3] Self-trapped optical beams in other, non-Kerr, nonlinear media have been also investigated during the past few years. Theoretical studies have found stable self-trapping of a two-dimensional beam in saturable self-focusing media,[4,5] and a recent study[6] reported a pair of spiraling solitons formed by the breakup of an optical vortex in such a medium. Another type of nonlinearity that permits self-trapping in both transverse dimensions is based on cascaded $\chi^{(2)}$ effects, in which a fundamental and a second-harmonic beam interact and trap each other.[7] Finally, guidance of optical beams by soliton-induced waveguides as a means of controlling light by light has been investigated experimentally for one-dimensional beams[8] and theoretically for one- and two-dimensional beams.[9]

Recently another type of soliton—the photorefractive spatial soliton[10–18]—has attracted much interest because it exhibits stable self-trapping in two transverse dimensions even with low optical power (microwatt/s). Photorefractive solitons are generally classified into three generic types: quasi-steady-state solitons,[10,11] photovoltaic solitons,[12] and steady-state screening solitons.[13–17] All these photorefractive solitons also induce waveguides in the volume of a bulk photorefractive medium. Photorefractive soliton-induced waveguides have been demonstrated for quasi-steady-state solitons,[18] photovoltaic solitons,[12] and dark-screening solitons.[17] Waveguides induced by photorefractive solitons are inherently different from those induced by Kerr-type solitons not only because they exist in two transverse dimensions but also with respect to their wavelength response. Since the response of photorefractive media is wavelength dependent, one can generate a soliton with a very weak beam and guide in it a much more intense beam of a wavelength at which the material is less photosensitive. This permits the steering and controlling of intense beams by weak (soliton) beams. This property does not exist for Kerr-type solitons because the Kerr nonlinearity must be far from any resonance and is therefore wavelength independent. Thus waveguides induced by Kerr-type solitons can guide only beams that are much weaker than the soliton beams.[8]

Photorefractive spatial screening solitons form when diffraction is balanced by photorefractive self-focusing effects. A bright screening soliton results from the spatially nonuniform screening of an externally applied field, which lowers the refractive index away from the center of the optical beam and forms an effective waveguide. This waveguide can guide another probe beam, possibly at a different wavelength (which is long enough to exclude intrinsic valence-band–conduction-band excitation), with a slightly different refractive index and electro-optic coefficient. Here we demonstrate what to our knowledge is the first experimental observation of circular waveguides induced by two-dimensional bright-solitons—in any nonlinear medium. The waveguides are induced by photorefractive screening solitons. We study their guiding properties and show that, when the waveguide is induced by a soliton whose peak intensity is of the order of the sum of the dark plus the background irradiances, it is a single-mode waveguide. However, when this intensity ratio increases, the soliton-induced waveguide starts to guide higher modes, with the number of guided modes increasing with the intensity ratio of the soliton.

The screening solitons are generated with an experimental setup similar to that of Ref. 16. We first generate a screening soliton in a 5.5-mm-long strontium barium niobate crystal (SBN:60) by launching a 1.5-μW extraordinarily polarized TEM_{00} beam of 488-nm wavelength along the crystalline a axis. An external voltage of 1900 V applied along the crystalline c axis between electrodes separated by 5.5 mm permits the formation of a 12-μm-wide (FWHM)

0146-9592/96/130931-03$10.00/0

circular (axially symmetric) screening soliton with an intensity ratio of 3. When the intensity ratio is varied to 120, support of the 12-μm soliton requires a higher voltage (2900 V) (in accordance with observations in Ref. 16). For optical guiding we use an extraordinarily polarized He–Ne beam of 633-nm wavelength (which serves as a probe beam) and focus it at the front face of the crystal at the same spot at which we launch the soliton beam. The difference in the indices of refraction at the center of the induced waveguide and its margins is 4.9×10^{-4} at intensity ratio 3 and 7.5×10^{-4} at ratio 120 [$|\Delta n|_{\max} = (1/2) n_b^3 r_{\text{eff}} V/l$, where $n_b = 2.35$ is the background refractive index and $r_{\text{eff}} = 220 \times 10^{-12}$ m/V is the electro-optic coefficient]. The corresponding numerical apertures of the waveguide are roughly 0.048 and 0.059 for intensity ratios 3 and 120, respectively. Therefore the difference between the angles of incidence of the soliton beam and the probe beam cannot be too large; otherwise, the critical angle (for guiding) is exceeded.

Beam profiles and photographs of the soliton, the probe beam guided by the soliton-induced waveguide, and both beams in the normal-diffraction regime are shown in Fig. 1. At zero voltage the soliton beam diffracts from 12-μm diameter (FWHM) at the input face [Fig. 1(a)] to 45 μm at the exit face of the crystal [Fig. 1(b)]. We then apply 2100 V across the crystal with intensity ratio 30, and a 12-μm two-dimensional soliton is formed [Fig. 1(c)]. A photograph of the soliton beam at the exit face of the crystal is shown in Fig. 1(d). We then launch a 15-μW 13-μm probe beam [Fig. 1(e)] into the soliton-induced waveguide. In the absence of the soliton-induced waveguide (or when the voltage is set to zero) the probe beam diffracts to 53 μm [Fig. 1(f)]. Note that the probe beam diffracts more than the soliton beam because the probe beam is of a longer wavelength. In the presence of the induced waveguide the probe beam propagates throughout the crystal, exhibiting good guidance, and leaves the crystal with a beam size of 12 μm, as shown in Fig. 1(g) and in the photograph, Fig. 1(h). From profiles of the guided beam at the crystal exit face and its far-field distribution (single lobe), it is evident that the probe beam is guided as the fundamental mode of the waveguide. Note the soliton stability and reshaping as observed by comparing the diffraction-beam profiles [Figs. 1(b) and 1(f)] with those of the soliton [Fig. 1(c)] and the guided (probe) beam [Fig. 1(g)]. We measure the output power in the probe beam and find that the coupling efficiency into the soliton-induced waveguide is ~85%, normalized to absorption ($\alpha = 0.21$ cm^{-1}) and Fresnel reflections. Figure 2 shows typical top-view photographs of the guided probe beam [Fig. 2(a)] within the soliton-induced waveguide and the naturally diffracting probe beam [Fig. 2(b)] in the absence of the soliton-induced waveguide.

We point out the significant difference between waveguides induced by steady-state screening solitons and those induced by quasi-steady-state solitons.[18] Quasi-steady-state solitons are transient in their nature; thus one has to shut the soliton beam off when it reaches its optimal diameter (before the screening process takes place) and then use the space-charge field that supports the induced waveguide for guiding. The space-charge field decays (slowly) owing to the dark conductivity and the photoconductivity set by the probe beam. Thus waveguiding induced by quasi-steady-state solitons is inevitably transient, as observed in Ref. 18. Waveguides induced by screening solitons, on the other hand, exist in steady state. Thus the steady-state soliton beam guides the probe beam, and the waveguide does not decay, provided that the soliton beam is on. When the soliton beam is shut off, the space-charge field decays slowly (as it does in quasi-steady-state soliton-induced waveguides). For this reason, steady-state screening solitons are excellent candidates for applications that require both programmable and nondecaying waveguides.

Elsewhere we investigated theoretically the guiding properties of screening solitons in one transverse dimension. We found that waveguides induced by a bright one-dimensional screening soliton can support a different number of guided modes, depending on the intensity ratio used to form the soliton. For a bright soliton, the higher the intensity ratio, the greater the number of guided modes supported by the soliton-induced waveguide. Here we investigate that principle for a two-dimensional waveguide induced by a circular two-dimensional soliton and find a similar trend. First, we generate a 12-μm two-dimensional screening soliton [Fig. 3(a)] with intensity ratio 120. Then we insert a horizontal thin glass into one

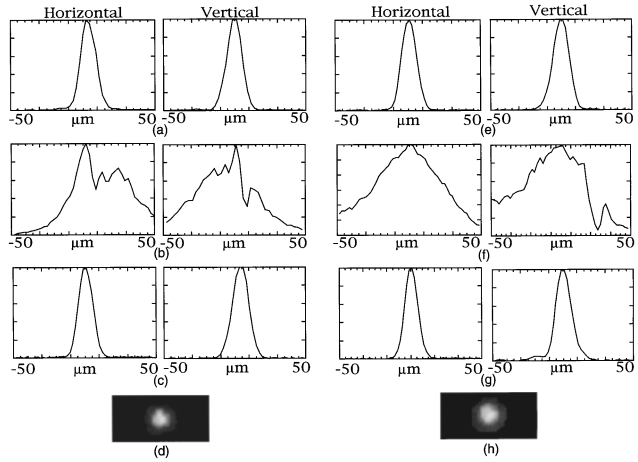

Fig. 1. (a) Horizontal and vertical profiles of the soliton beam at the crystal input face; (b) and (c) are the diffraction profiles and the soliton profiles, respectively, and (d) is a photograph of the soliton (all taken at the exit face). Horizontal and vertical profiles of the He–Ne probe beam at (e) the input face; (f) and (g) are the diffraction and guided profiles, respectively, and (h) is a photograph of the guided beam (all taken at the exit face).

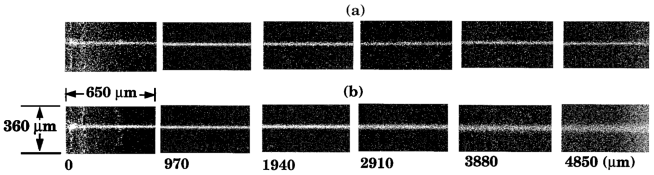

Fig. 2. Top-view photographs of (a) the guided and (b) the nonguided (in the absence of the soliton-induced waveguide) He–Ne probe beam.

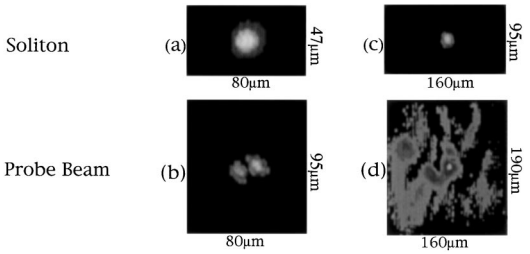

Fig. 3. Photographs of (a) a soliton with intensity ratio 120, (b) the guided He–Ne TEM_{10} mode, (c) a soliton with intensity ratio 3, and (d) the nonguided He–Ne beam whose input beam is the same as that of (b), all taken at the exit face of the crystal.

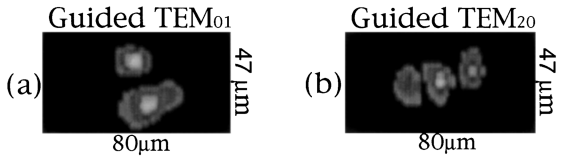

Fig. 4. Photographs of the guided He–Ne (a) TEM_{01} and (b) TEM_{20} modes, taken at the exit face of the crystal.

half of the probe beam and introduce a vertical dark notch at the center of that beam. We tilt the glass, generating a π-phase jump to simulate the TEM_{10} mode (in a manner similar to that used to excite dark solitons[11,18]), and launch this probe beam into the soliton-induced waveguide. The photograph of the probe beam at the crystal exit face [Fig. 3(b)] proves that a probe beam of TEM_{10} mode can be guided by a waveguide induced by a soliton of intensity ratio 120 (with a coupling efficiency of ~40%). We then change the intensity ratio to 3, reduce the voltage accordingly,[16] and again generate an axially symmetric soliton [Fig. 3(c)] of the same size (12 μm). Now the TEM_{10} probe beam cannot be guided by the soliton-induced waveguide, as observed from Fig. 3(d) [note that Figs. 3(c) and 3(d) have a larger scale]. Only a small portion of the TEM_{10} probe beam is confined inside the soliton-induced waveguide (by a weak excitation of the fundamental mode), and the rest spreads as widely as does the naturally diffracting beam in the absence of the soliton-induced waveguide. Readjusting the probe beam to be TEM_{00} mode by removing the glass, we find that the probe beam can be well guided inside the soliton-induced waveguide with an intensity ratio of either 120 or 3. Thus a waveguide induced by a screening soliton of intensity ratio 3 is a single-mode waveguide, whereas a waveguide induced by a soliton of intensity ratio 120 can guide at least two modes.

We then rotate the symmetry of the probe beam to generate a TEM_{01} mode (by inserting a vertical glass slide into the probe beam that generates a horizontal dark notch) and observe that the waveguide induced by a soliton at intensity ratio 120 can also guide a TEM_{01} beam [Fig. 4(a)] with a coupling efficiency of 40%. Thus the waveguide is circularly symmetric, as is the soliton that forms it. We then excite higher modes in the same waveguide. Using two glass slides sequentially, we generate a TEM_{20} probe beam and find that it can be guided by the same waveguide [Fig. 4(b)] with a coupling efficiency of 33%. In general, the higher the ratio of the peak soliton intensity to the sum of the dark and background irradiances, the more modes that can be guided. Nevertheless, the soliton beams themselves are still the fundamental guided mode of the waveguides they induce.

In summary, we have demonstrated what we believe is the first observation of soliton-induced circular waveguides in a bulk nonlinear medium. The waveguides induced by two-dimensional photorefractive screening solitons can guide both the soliton beams that induce them and other probe beam, possibly at different wavelengths. We show that the number of guided modes increases with increasing intensity ratio of the soliton that induces them and that single-mode waveguides are generated at low intensity ratios.

M. Segev gratefully acknowledges the support of a Sloan Fellowship and of Hughes Research Laboratories.

References

1. R. Y. Chiao, E. Garmire, and C. H. Townes, Phys. Rev. Lett. **13,** 479 (1964).
2. J. S. Aitchinson, A. M. Weiner, Y. Silberberg, M. K. Oliver, J. L. Jackel, D. E. Leaird, E. M. Vogel, and P. W. Smith, Opt. Lett. **15,** 471 (1990).
3. P. L. Kelley, Phys. Rev. Lett. **15,** 1005 (1965).
4. A. W. Snyder, D. J. Mitchell, L. Poladian, and F. Ladouceur, Opt. Lett **16,** 21 (1991).
5. J. M. Soto-Crespo, D. R. Heatler, E. M. Wright, and N. N. Akhmediev, Phys. Rev. A **44,** 636 (1991); M. Karlsson, Phys. Rev. A **46,** 2726 (1992).
6. V. Tikhonenko, J. Christou, and B. Luther-Davies, J. Opt. Soc. Am. B **12,** 2046 (1995).
7. W. E. Torruellas, Z. Wang, D. J. Hagan, E. W. Van Stryland, G. I. Stegeman, L. Torner, and C. R. Menyuk, Phys. Rev. Lett. **74,** 5036 (1995).
8. R. De La Fuente, A. Barthelemy, and C. Froehly, Opt. Lett. **16,** 793 (1991).
9. A. W. Snyder, D. J. Mitchell, and Y. S. Kivshar, Mod. Phys. Lett. B **9,** 1479 (1995).
10. M. Segev, B. Crosignani, A. Yariv, and B. Fischer, Phys. Rev. Lett. **68,** 923 (1992).
11. G. Duree, J. L. Shultz, G. Salamo, M. Segev, A. Yariv, B. Crosignani, P. DiPorto, E. Sharp, and R. Neurgaonkar, Phys. Rev. Lett. **71,** 533 (1993); **74,** 1978 (1995).
12. G. C. Valley, M. Segev, B. Crosignani, A. Yariv, M. M. Fejer, and M. Bashaw, Phys. Rev. A **50,** R4457 (1994); M. Taya, M. Bashaw, M. M. Fejer, M. Segev, and G. C. Valley, Phys. Rev. A **52,** 3095 (1995).
13. The steady-state self-focusing effect was first observed by M. D. Iturbe-Castillo, P. A. Marquez-Aguilar, J. J. Sanchez-Mondragon, S. Stepanov, and V. Vysloukh, Appl. Phys. Lett. **64,** 408 (1994).
14. M. Segev, G. C. Valley, B. Crosignani, P. DiPorto, and A. Yariv, Phys. Rev. Lett. **73,** 3211 (1994); M. Segev, M. Shih, and G. C. Valley, J. Opt. Soc. Am. B **13,** 706 (1996).
15. D. N. Christodoulides and M. I. Carvalho, J. Opt. Soc. Am. B **12,** 1628 (1995).
16. M. Shih, M. Segev, G. C. Valley, G. Salamo, B. Crosignani, and P. DiPorto, Electron. Lett. **31,** 826 (1995); Opt. Lett. **21,** 324 (1996).
17. Z. Chen, M. Mitchell, M. Shih, M. Segev, M. Garrett, and G. C. Valley, Opt. Lett. **21,** 629 (1996); Z. Chen, M. Mitchell, and M. Segev, Opt. Lett. **21,** 716 (1996).

18. M. Morin, G. Duree, G. Salamo, and M. Segev, Opt. Lett. **20,** 2066 (1995).